COMPOSITE TUBES WITH NOVEL BEND-TWIST COUPLING

S.E. Rohde, AK. Jonnalagadda, A.S. Savant, P.G. Ifju and B.V. Sankar[1]

Department of Mechanical and Aerospace Engineering, University of Florida
P.O. Box 116250, Gainesville, Florida 32611, USA
Email[1]: sankar@ufl.edu, web page: http://www.mae.ufl.edu

Keywords: Bend-twist coupling, Composite tube, Extension-shear coupling, Shear-center, Torsion

ABSTRACT

An analytical model for composite tubes possessing bend-twist coupling is derived. The tubes experience torsion when loaded in pure bending and bending when loaded in pure torsion. This is characterized by an off-axis shear center. A novel design for creating this coupling effect is described. Analytical expressions for the shear center distance are derived. Finite element analysis using shell elements is performed. The agreement in the results, especially the shear–center distance, is excellent. Experimental testing provided a second means of verification with good agreement. It is found that the location of the shear-center is independent of the shaft radius but proportional to the length of the tube. These properties are fundamentally different from the more common case of bend-twist coupling resulting from unbalanced shear flows in asymmetric cross-section of isotropic beams. The coefficient of mutual influence of the composite material affects the shear-center as well.

1 INTRODUCTION

Tubular structures are efficient when the loading is a combination of bending and torsion. Tubes made of homogeneous materials are axisymmetric and hence there will be no coupling between flexural and torsional deformations resulting from unbalanced shear flows. There are applications, however, where a transverse force has to be applied to a tubular lever eccentrically without resulting in twisting. Examples include golf clubs or the torsion bars in automobiles. Taking advantage of elastic coupling in anisotropic materials, shear centers at a distance from the geometric centroid can be achieved. Figure 1 illustrates an example of an eccentric loading that does not cause torsion because the load acts at the shear center.

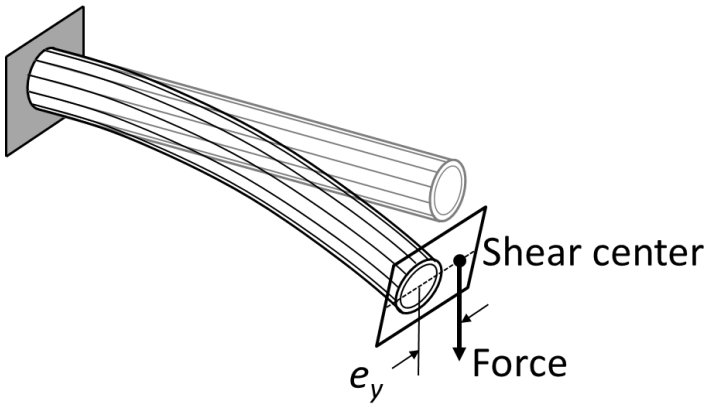

Figure 1: Composite tube loaded through an off axis shear center. The longitudinal lines indicate absence of rotation, not fiber orientation.

Recently, Rohde et al. [1, 2] have proposed a novel composite tube design which is intended to yield bend-twist coupling. The design is described in detail in the Results and Discussions section. In this paper we present a beam theory for an anisotropic composite tube subjected to combined bending and torsion to characterize the bend-twist coupling in the aforementioned tube by Rohde et al. The analytical results are verified using finite element analysis and experimental testing. A simple formula is derived for the shear center distance - distance of shear center from the axis of the tube. This can be used to optimize the design to achieve the desired shear center distance.

It is worth pointing out that Rao and Chan [3] have developed an analytical model for the analysis of laminated tubes subjected to both an axial force and a twisting moment. They modified the lamination theory to account for the ply stiffness of a differential element along the circumference of the tube using the appropriate transformation. Then the stiffness of the tube was obtained by integrating the stiffness around the circumference. In the present approach, suitable assumptions are made about the deformation of the tube and the shear stress distribution. This leads to an independent beam theory for composite tubes.

2 ANALYTICAL MODEL

2.1 A beam theory for combined bending and torsion of tubes

Consider a thin-walled tube with the tube axis parallel to the *x*-axis. The mean radius of the tube is *R* and the wall thickness *h*<<*R*. The tube is made of two anisotropic materials - top half $(0 < \theta < \pi)$ is made of Material 1 and the bottom half $(\pi < \theta < 2\pi)$ is of Material 2. We assume that the tube is in a state of plane stress normal to the radial direction *n* (see Fig. 2) such that $\sigma_{nn} = \tau_{nx} = \tau_{ns} = 0.$ Furthermore, we assume the hoop or circumferential stress $\sigma_{ss} = 0.$ Thus the two significant stresses are the axial stress σ_{xx} and the shear stress τ_{xs}. We assume that the tube deforms such that plane sections remain plane and normal to the tube axis as in Bernoulli-Euler beam theory. As will be seen later this assumption works well for the thin-walled, long tubes considered in this study. Then the displacement field can be written as

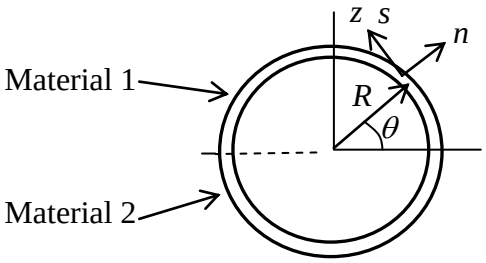

Figure 2: Cross section of the tube and the coordinate system.

$$\begin{aligned} u(x,y,z) &= u_0(x) - y\frac{dv_0}{dx} - z\frac{dw_0}{dx} \\ v(x,y,z) &= v_0(x) \\ w(x,y,z) &= w_0(x) \end{aligned} \tag{1}$$

where u_0, v_0 and w_0 are the deflections of the beam axis. The axial strain takes the form

$$\begin{aligned}\varepsilon_{xx} &= \frac{\partial u}{\partial x} \\ &= \frac{\partial u_0}{\partial x} - y\frac{d^2 v_0}{dx^2} - z\frac{d^2 w_0}{dx^2} \\ &= \varepsilon_{xo} + y\kappa_y + z\kappa_z\end{aligned} \tag{2}$$

where κ_y and κ_z are the curvatures. We do not make any specific assumption about the rotation of the cross section except the average rotation of the cross-section about the *x*-axis is denoted by ψ_x. But we assume the shear stress is uniform and given by

$$\tau_{xs} = \frac{T}{2\pi R^2 h} = \tau_0 \tag{3}$$

where *T* is the torque acting on a cross section.

Though the above assumption about the shear stress distribution seems to be trivial, it is important in the present context. In traditional torsion theories the plane cross section of the tube is assumed to rotate as a rigid body leading to constant γ_{xs} shear strain along the circumference of the tube. When the material is also homogenous it leads to constant shear stress τ_{xs} which is consistent with the assumption in Eq.(3) above. However, when the tube is made of two different materials, the shear stress τ_{xs} has to be continuous at the interface between the two materials, but the shear strain γ_{xs} does not have to be continuous at the interface. That is why no specific kinematic assumption is made regarding the rotation of the tube.

The constitutive relation for both materials can be written in the form [4]

$$\begin{Bmatrix}\varepsilon_{xx} \\ \gamma_{xs}\end{Bmatrix} = \begin{bmatrix}\frac{1}{E_x} & \frac{\eta_{xs,x}}{G_{xs}} \\ \frac{\eta_{x,xs}}{E_x} & \frac{1}{G_{xs}}\end{bmatrix}\begin{Bmatrix}\sigma_{xx} \\ \tau_{xs}\end{Bmatrix} = \begin{bmatrix}\bar{S}_{11} & \bar{S}_{16} \\ \bar{S}_{16} & \bar{S}_{66}\end{bmatrix}\begin{Bmatrix}\sigma_{xx} \\ \tau_{xs}\end{Bmatrix} \tag{4}$$

where *E* and *G* are Young's modulus and shear modulus, respectively, η is the coupling term called coefficient of mutual influence of the material, and $\bar{S}_{ij}$ are the transformed compliance terms of the lamina . Then from (2), (3) and (4) we obtain

$$\begin{aligned}\sigma_{xx} &= E_x\varepsilon_{xx} - \eta_{x,xs}\tau_{xs} \\ &= E_x\left(\varepsilon_{x0} + y\kappa_y + z\kappa_z\right) - \eta_{x.xs}\tau_0\end{aligned} \tag{5}$$

The force and bending moment resultants are defined as

$$\begin{aligned}\left(P, M_y, M_z\right) &= \int_A \sigma_{xx}\left(1, z, -y\right)dA \\ &= \int_0^{2\pi} \sigma_{xx}\left(1, R\sin\theta, -R\cos\theta\right)Rhd\theta\end{aligned} \tag{6}$$

where the integration is performed over the cross section of the tube. Substituting for σ_{xx} from (5) we obtain

$$\begin{aligned}\left(P, M_y, M_z\right) &= \int_0^{\pi}\left[E_x^{(1)}\left(\varepsilon_{x0} + R\cos\theta\,\kappa_y + R\sin\theta\,\kappa_z\right) - \eta_{x,xs}^{(1)}\tau_0\right]\left(1, R\sin\theta, -R\cos\theta\right)Rhd\theta \\ &+ \int_{\pi}^{2\pi}\left[E_x^{(2)}\left(\varepsilon_{x0} + R\cos\theta\,\kappa_y + R\sin\theta\,\kappa_z\right) - \eta_{x,xs}^{(2)}\tau_0\right]\left(1, R\sin\theta, -R\cos\theta\right)Rhd\theta\end{aligned} \tag{7}$$

where the superscripts (1) and (2) refer to the two materials. Performing the integration we obtain relations between the force and moment resultants and deformations:

$$\begin{bmatrix} \bar{E}_x A & \frac{AR}{\pi}\Delta E_x \\ \frac{AR}{\pi}\Delta E_x & \bar{E}_x I \end{bmatrix}\begin{Bmatrix}\varepsilon_{x0} \\ \kappa_z\end{Bmatrix} = \begin{Bmatrix} P \\ M_y\end{Bmatrix} + \begin{Bmatrix} A\bar{\eta}_{x,xs} \\ 2R^2 h\,\Delta\eta_{x,xs}\end{Bmatrix}\tau_0$$

$$\bar{E}_x I\kappa_y = -M_z \tag{8}$$

In the above equations $\bar{E}_x$ is the average Young's modulus given by $\bar{E}_x = \left(E_x^{(1)} + E_x^{(2)}\right)/2$, ΔE_x is the difference in the Young's moduli, $\Delta E_x = \left(E_x^{(1)} - E_x^{(2)}\right)$. Similarly $\bar{\eta}_{x,xs} = \left(\eta_{x,xs}^{(1)} + \eta_{x,xs}^{(2)}\right)/2$ and $\Delta\eta_{x,xs} = \left(\eta_{x,xs}^{(1)} - \eta_{x,xs}^{(2)}\right)$, $A = 2\pi Rh$ is the cross sectional area and I is the second moment of inertia given by $I = \pi R^3 h$. Equation (8) can be inverted to obtain

$$\begin{Bmatrix}\varepsilon_{x0} \\ \kappa_z\end{Bmatrix} = \frac{1}{K}\begin{bmatrix} \bar{E}_x I & \frac{-AR}{\pi}\Delta E_x \\ \frac{-AR}{\pi}\Delta E_x & \bar{E}_x A \end{bmatrix}\left(\begin{Bmatrix} P \\ M_y\end{Bmatrix} + \begin{Bmatrix} \bar{\eta}_{x,xs}/R \\ \Delta\eta_{x,xs}/\pi\end{Bmatrix}T\right)$$

$$\kappa_y = -M_z/\bar{E}_x I \tag{9}$$

$$\text{where } K = \bar{E}_x^2 AI - \left(\frac{AR\Delta E_x}{\pi}\right)^2$$

Thus one can calculate the deformations from the force and moment resultants. The deflections can be obtained by integrating the strains and curvatures as will be shown in the examples. From eq. (9) it is evident that a torque *T* can result in curvature κ_z causing deflection of the tube in the *z*-direction. It is interesting to note that the torque *T* does not cause curvature κ_y and this is due to symmetry of the cross section about the *z*-axis.

2.2 Angle of twist

The average torsional rotation ψ_x is calculated as follows. Let us define the average unit angle of twist $\bar{\phi} = d\psi_x/dx$. The shear strain can be written as

$$\begin{aligned}\gamma_{xs} &= \frac{\partial u_s}{\partial x} + \frac{1}{R}\frac{\partial u}{\partial\theta} \\ &= R\phi + \frac{1}{R}\frac{\partial u}{\partial\theta}\end{aligned} \tag{10}$$

where u_s is the displacement at a point in the tangential direction. The first term on the RHS of the above equation has been written as $\partial u_s / \partial x = R\phi$, where $\phi(s)$ is the unit angle of twist at a given location *s*. Then the average unit angle of twist is obtained as

$$\begin{aligned}\bar{\phi} &= \frac{1}{2\pi}\int_0^{2\pi}\phi\, d\theta \\ &= \frac{1}{2\pi}\int_0^{2\pi}\frac{\gamma_{xs}}{R}\,d\theta - \frac{1}{2\pi}\int_0^{2\pi}\frac{1}{R^2}\frac{\partial u}{\partial \theta}\,d\theta \\ &= \frac{1}{2\pi R}\int_0^{2\pi}\gamma_{xs}\,d\theta\end{aligned} \tag{11}$$

Note the second integral in the above equation vanishes as it is the contour integration of an exact differential. From the constitutive relation (4) the shear strain at a point on the circumference of the tube can be written in terms of stresses as

$$\gamma_{xs} = \frac{\eta_{x,xs}}{E_x}\sigma_{xx} + \frac{\tau_{xs}}{G_{xs}} \tag{12}$$

From (12) it is clear that the shear strain γ_{xs} will not be continuous across the interface between Materials 1 and 2 because of the difference in elastic constants and also due to the difference in bending stress σ_{xx}. That is why we calculate the average rotation by integrating the unit angle of twist along the circumference of the tube.

Substituting for σ_{xx} from (5) into (12) and then substituting for γ_{xs} from (12) into (11) the average unit angle of twist can be derived as

$$\bar{\phi} = \frac{\bar{\eta}_{x,xs}}{R}\varepsilon_{x0} + \frac{\Delta\eta_{x,xs}}{\pi}\kappa_z + \frac{1}{R}\left[-\left(\overline{\frac{\eta_{x,xs}^2}{E_x}}\right) + \frac{1}{\bar{G}_{xs}}\right]\tau_0 \tag{13}$$

where

$$\begin{aligned}\left(\overline{\frac{\eta_{x,xs}^2}{E_x}}\right) &= \frac{1}{2}\left(\frac{\left(\eta_{x,xs}^{(1)}\right)^2}{E_x^{(1)}} + \frac{\left(\eta_{x,xs}^{(2)}\right)^2}{E_x^{(2)}}\right) \\ \frac{1}{\bar{G}_{xs}} &= \frac{1}{2}\left(\frac{1}{G_{xs}^{(1)}} + \frac{1}{G_{xs}^{(2)}}\right)\end{aligned} \tag{14}$$

Once the deformations ε_{x0} and κ_z are calculated from (9), the unit angle of twist can be calculated using (13). Using eq. (9) one can express ε_{x0} and κ_z in eq. (13) in terms of force and moment resultants *P*, M_y and *T*. Thus it is obvious that a bending moment M_y about the *y*-axis can cause twisting in the tube demonstrating the bend-twist coupling.

2.3 Shear stress due to transverse force

The present formulation is based on Euler-Bernoulli beam theory and hence the shear stresses due to transverse forces V_y and V_z are not accounted for. Only the shear stresses due to the torque are included. The transverse shear stresses can be recovered from $\sigma_{xx}(x)$ using the equilibrium equation

as in classical mechanics of materials. First consider the shear force V_z. The bending moment created will be M_y and they are related by $dM_y/dx = V_z$. Integrating the equilibrium equation we obtain

$$\frac{\partial \sigma_{xx}}{\partial x} + \frac{\partial \tau_{xs}}{\partial s} = 0 \Rightarrow \tau_{xs}(s) = \tau_{xs}(0) - R\int_0^\theta \frac{\partial \sigma_{xx}}{\partial x} d\theta \tag{15}$$

Substituting for σ_{xx} from (5) we obtain

$$\tau_{xs}(s) = \tau_{xs}(0) - R\int_0^\theta \frac{\partial\left(E_x\left(\varepsilon_{x0} + z\kappa_z\right)\right)}{\partial x} d\theta \tag{16}$$

Again substituting for ε_{x0} and κ_z from (9) in terms of M_y and using $dM_y/dx = V_z$:

$$\tau_{xs}(s) = \tau_{xs}(0) - \frac{V_z R^2 A}{K}\int_0^\theta E_x\left(\frac{-\Delta E_x}{\pi} + \bar{E}_x \sin\theta\right) d\theta \tag{17}$$

Performing the above integration we obtain an expression for shear stresses due to V_z:

$$\begin{aligned}\tau_{xs}(\theta) &= \tau_{xs}(0) - \frac{V_z R^2 A E_x^{(1)}}{K}\left(\frac{-\Delta E_x}{\pi}\theta + \left(-\cos\theta + 1\right)\bar{E}_x\right), \quad 0 < \theta < \pi \\ &= \tau_{xs}(0) - \frac{2V_z R^2 A E_x^{(1)} E_x^{(2)}}{K} - \frac{V_z R^2 A E_x^{(2)}}{K}\left(\frac{-\Delta E_x}{\pi}\left(\theta - \pi\right) - \left(1 + \cos\theta\right)\bar{E}_x\right), \quad \pi < \theta < 2\pi\end{aligned} \tag{18}$$

Similarly we can derive an expression for transverse shear stress due to shear force V_y as:

$$\tau_{xs}(s) = \tau_{xs}(0) - R\int_0^\theta \frac{\partial\left(E_x y \kappa_y\right)}{\partial x} d\theta \tag{19}$$

Substituting for κ_y from (9) and using $dM_z/dx = -V_y$:

$$\begin{aligned}\tau_{xs}(\theta) &= \tau_{xs}(0) - \frac{V_y R^2}{\bar{E}_x I}\int_0^\theta E_x \cos\theta d\theta \\ &= \tau_{xs}(0) - \frac{V_y R^2 E_x^{(1)} \sin\theta}{\bar{E}_x I}, \; 0 < \theta < \pi \\ &= \tau_{xs}(0) - \frac{V_y R^2 E_x^{(2)} \sin\theta}{\bar{E}_x I}, \; \pi < \theta < 2\pi\end{aligned} \tag{20}$$

3 APPLICATION TO FIBER COMPOSITE TUBES

3.1 Tube made of an anisotropic material with different orientations

Recently Rohde et al. [2] have proposed a novel composite tube design which exhibits the bend-twist coupling described in the previous section (see Fig. 3). In this design two different lay-ups or fiber orientations are used for each half of the circular tube. Assume the tube is made of a unidirectional fiber composite. The fiber-angle is the angle between the fiber direction (1-direction) and the *x*-axis. It is assumed $+\alpha$ for the top half of the tube (Material 1) and $-\alpha$ for the bottom half (Material 2) as shown in Fig. 3 and Fig. 4.

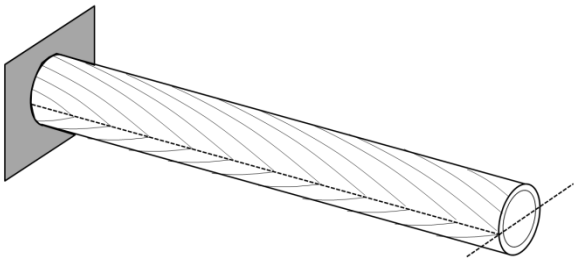

Figure 3: An isometric view of the composite tube showing different fiber orientations on the top and bottom halves.

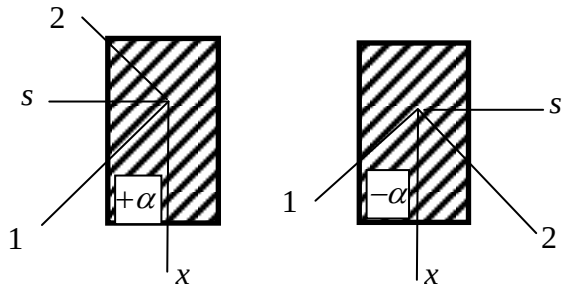

Figure 4: The left figure shows the top half of the tube with fiber orientation +α. Right figure shows the bottom half (fiber angle -α) viewed from the top. Note the difference in the direction of circumferential direction (*s*-axis) in the two figures.

The elastic constants in the *x*-*s* coordinate system can be obtained from the orthotropic engineering elastic constants E_1, E_2, G_{12} and ν_{12} as follows [4]:

$$\begin{aligned}
&\frac{1}{E_x} = \frac{1}{E_1} l^4 + \left(-\frac{2\nu_{12}}{E_1} + \frac{1}{G_{12}} \right) l^2 m^2 + \frac{1}{E_2} m^4 \\
&\frac{1}{G_{xs}} = 2\left(\frac{2}{E_1} + \frac{2\nu_{12}}{E_1} + \frac{4\nu_{12}}{E_1} - \frac{1}{G_{12}} \right) l^2 m^2 + \frac{1}{G_{12}} \left(l^4 + m^4 \right) \\
&\frac{\eta_{x,xs}}{E_x} = \left(\frac{2}{E_1} + \frac{2\nu_{12}}{E_1} - \frac{1}{G_{12}} \right) l^3 m + \left(-\frac{2\nu_{12}}{E_1} - \frac{2}{E_2} + \frac{1}{G_{12}} \right) l m^3 \\
&l = \cos\alpha, \quad m = \sin\alpha
\end{aligned} \tag{21}$$

It is obvious from the above relations that for the present example

$$\begin{aligned}
&E_x^{(1)} = E_x^{(2)} = \bar{E}_x, \quad \Delta E_x = 0, \; G_{xs}^{(1)} = G_{xs}^{(2)} = \bar{G}_{xs}, \; \Delta G_{xs} = 0 \\
&\eta_{x,xs}^{(1)} = -\eta_{x,xs}^{(2)}, \quad \bar{\eta}_{x,xs} = 0, \quad \Delta\eta_{x,xs} = 2\eta_{x,xs}^{(1)}, \; \overline{\left(\frac{\eta_{x,xs}^2}{E_x} \right)} = \frac{\left(\eta_{x,xs}^{(1)} \right)^2}{\bar{E}_x}
\end{aligned} \tag{22}$$

Then Eqs. (8) and (13) can be simplified as

$$\begin{aligned}
\bar{E}_x A\varepsilon_{x0} &= P \\
\bar{E}_x I\kappa_z &= M_y + 4R^2 h\eta_{x,xs}^{(1)}\tau_0 \\
\bar{E}_x I\kappa_y &= -M_z \\
\bar{\phi} &= \frac{2\eta_{x,xs}^{(1)}}{\pi}\kappa_z + \frac{1}{R}\left[\frac{1}{\bar{G}_{xs}} - \frac{\left(\eta_{x,xs}^{(1)}\right)^2}{\bar{E}_x}\right]\tau_0
\end{aligned} \tag{23}$$

From the above relations (2nd and 4th equations) one can note the coupling between the bending moment M_y and the torque T. The two relevant equations can be written as

$$\begin{aligned}
\kappa_z &= \frac{M_y}{\bar{E}_x I} + \frac{2\eta_{x,xs}^{(1)}}{\pi\bar{E}_x I}T \\
\bar{\phi} &= \frac{4\eta_{xs,x}^{(1)}}{\pi\bar{G}_{xs}J}M_y + \left(1+\left(\frac{8}{\pi^2}-1\right)\eta_{x,xs}^{(1)}\eta_{xs,x}^{(1)}\right)\frac{T}{\bar{G}_{xs}J}
\end{aligned} \tag{24}$$

In deriving the above relations we have used $T = 2\pi R^2 h\tau_0$, $J = 2I = 2\pi R^3 h$, and the symmetry relation $\eta_{x,xs}/E_x = \eta_{xs,x}/G_{xs}$. The shear stresses due to the transverse force F_z can be obtained from (18) using $\Delta E_x = 0$ and $E_x^{(1)} = E_x^{(2)} = E_x$:

$$\tau_{xs}(\theta) = \tau_{xs}(0) + \frac{V_z R^2}{I}\left(\cos\theta - 1\right) \tag{25}$$

Note that the shear stress expression is the same for both top and bottom halves of the tube. The constant $\tau_{xs}(0)$ can be evaluated from the fact that the moment of the shear stresses about the center should vanish as the force F_z is applied at the center. The final expression for shear stress takes the form

$$\tau_{xs}(\theta) = \frac{V_z R^2}{I}\cos\theta = \frac{V_z R}{I}y \tag{26}$$

Thus the shear stress distribution will be symmetric about the z-axis such that $\tau_{xs}(y) = \tau_{xs}(-y)$. Thus the shear flow will be in the counter clockwise direction on the right half of the tube (y>0) and in the clockwise direction in the left half (y<0). The shear stresses will not contribute to rotation about the x-axis as the material is also symmetric about the z-axis.

3.2 Shear center

Consider a cantilevered tube clamped at x=0. First we will consider the case where the tube is subjected to a force F_z at the tip x=L. The force is such that the line of action is through the center of the tube. The bending moment distribution is given by $M_y(x) = -F_z(L-x)$. The tip rotation about the x-axis can be obtained from the second of Eq.(24):

$$\frac{d\psi_x}{dx} = \bar{\phi} = \frac{4\eta_{xs,x}^{(1)}}{\pi\bar{G}_{xs}J}F_z(x-L) \tag{27}$$

Integrating the above equation and noting $\psi_x(0) = 0$ we obtain the tip rotation ψ_x^F due the transverse force F_z as

$$\psi_x^F = \frac{-2\eta_{xs,x}^{(1)}}{\pi \bar{G}_{xs} J} F_z L^2 \tag{28}$$

From (24) the rotation ψ_x^T due to torque T can be derived as

$$\psi_x^T = \left(1+\left(\frac{8}{\pi^2}-1\right)\eta_{x,xs}^{(1)}\eta_{xs,x}^{(1)}\right)\frac{TL}{\bar{G}_{xs}J} \tag{29}$$

The location of the shear center can be derived as follows. Let the shear center distance – distance of the shear center from the tube axis – be denoted by e_y (Fig. 5). That is, if the transverse force F_z is applied at the shear center it would not produce any twisting of the tube, as the torque produced by the eccentric loading, F_z e_y, would cause an angle of twist equal in magnitude but opposite in direction to that produced by the force F_z. Then,

$$\psi_x^F = -\frac{\psi_x^T}{T}\left(F_z e_y\right) \Rightarrow e_y = \frac{-\left(\psi_x^F / F_z\right)}{\left(\psi_x^T / T\right)} \tag{30}$$

Substituting from (28) and (29) in the above equation, the shear center distance can be written in a non-dimensional form as

$$\frac{e_y}{L} = \frac{-\left(\psi_x^F / F_z\right)}{\left(\psi_x^T / T\right)L} = \frac{2\eta_{xs,x}^{(1)}}{\pi\left(1+\left(\frac{8}{\pi^2}-1\right)\eta_{x,xs}^{(1)}\eta_{xs,x}^{(1)}\right)} \tag{31}$$

From (23) we note that the bending moment M_z due to a transverse force F_y will not cause any twisting. Hence the shear center will be on the y-axis at a distance e_y from the center of the tube.

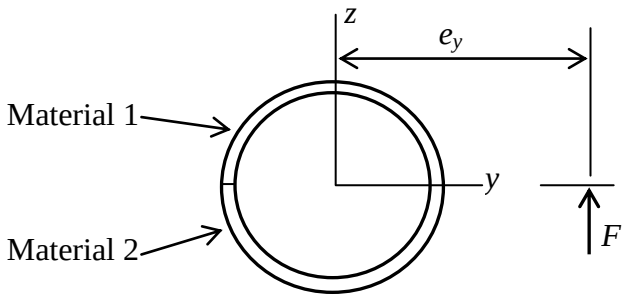

Figure 55: Shear Center for a tube made of an anisotropic material with different orientation of the principal material axis in the top and bottom halves of the tube as shown in Fig. 3.

We have already shown that the transverse shear stresses due to the force F_z do not contribute to the rotation due to symmetry of the across section about the z-axis. Thus we note the eccentricity of the shear center in the present case is due do the extension-shear coupling of the material. In homogeneous beams the eccentricity of the shear center is due to asymmetry of the cross section, *e.g.*, a C-channel. That is why the shear center location in the present case is independent of the radius R, but proportional to the tube length L and the coefficients of mutual influence η.

3.3 Laminated composite tubes

In most applications the tube has to be made of multiple plies with different fiber orientations to achieve a given bending stiffness, torsional stiffness and desired bend-twist coupling. In that case the laminated tube can be modeled as a tube with an equivalent anisotropic material. The compliance

matrix $\left[\bar{S}\right]$(see Eq. (4) above) of such an equivalent material can be obtained from the in-plane stiffness [*A*] of the laminate as follows [4]:

$$\left[\bar{S}_{eq}\right] = h\left[A\right]^{-1} \tag{32}$$

where *h* is the laminate thickness. It should be noted that the above idealization is valid only for thin-walled tubes such that *h*/*R*<<1.

4 FINITE ELEMENT ANALYSIS

The commercial finite element software Abaqus was used for computational analysis of aforementioned tubes. Eight-node doubly curved thick shell elements (S8R Element) were used to model the tubes. This element has six DOFs per node. About 30 elements were used along the circumference of the tube. The number of elements in the length direction was such that the aspect ratio of elements is approximately equal to unity. That is, the elements were almost square in shape. In the examples considered the tube was fixed at one end by setting all degrees of freedom equal to zero. At the free end, a reference node was created at the center of the tube and it was connected to the circumferential nodes using multipoint constraints. The transverse force and the couple were applied at the reference node.

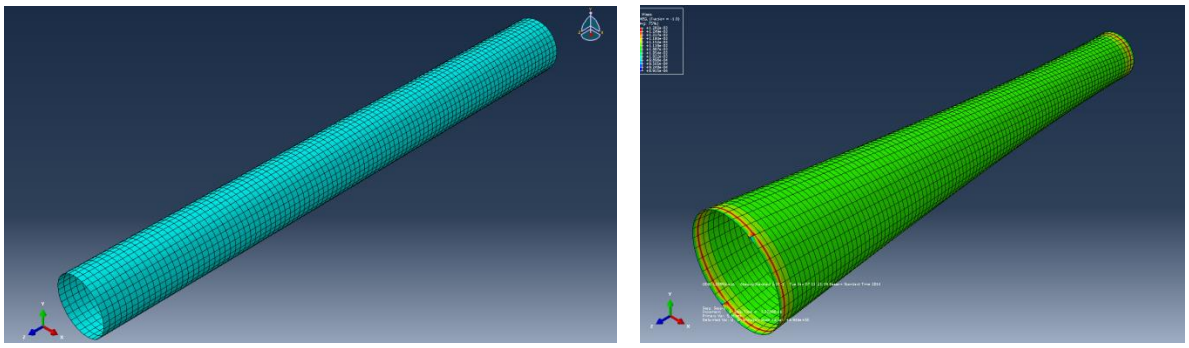

Figure 6: (a) FE mesh of the composite tube; (b) deformed shape after subjected to a torque at the tip. Note that the circumferential expansion of the tube is exaggerated in the figure.

5 RESULTS AND DISCUSSION

All examples below are concerned with a cantilevered tube of length *L*, mean radius *R*=10 mm and wall thickness *h*=2 mm. The tapered tube's radius varies from 5 mm at the fixed end to 15 mm at the free end.

5.1 Example 1A- one anisotropic material

The laminate configuration or lay-up is denoted by $\left[20^*\right]$. The superscript* denotes that for the top half of the tube $\alpha = +20^{\circ}$ and for the bottom half $\alpha = -20^{\circ}$ (see Fig. 3). The elastic constants are: E_1=138 GPa; E_2=9 GPa; G_{12}=6.9 GPa and $\nu_{12} = 0.3$. Tubes of two different lengths, 200 and 300 mm, were considered to demonstrate the length-dependence of shear center location. Two different forces were considered: a transverse tip force F_z applied at the center of the tube and a torque *T*. In Table 1 the FE results are compared with that obtained form the analytical method. It can be noted that the agreement for deflection, rotation and the shear center disctance are excellent. Furthermore, the ratio e_y/L does not change at all for the two different lengths of the tube.

Table 1: Results for tubes made of one orthotropic material but with opposite fiber orientations in the top and bottom halves. The top half of the tube consists of [+20] layers and the bottom half of [-20] layers.

Length L (mm)	Load F_z (N) T (N-mm)	Tip deflection $w_0(L)$ $\left(10^{-3}\text{ mm}\right)$		Tip rotation $\psi_x(L)$ (10^{-6} Radians)		Shear Center e_y/L	
		FEA	Analytical	FEA	Analytical	FEA	Analytical
200	F_z = 1	9.162	9.211	77.21	78.70	0.202	0.202
	T = 1	77.14	78.71	1.915	1.951		
300	F_z = 1	30.71	31.11	174.0	177.0	0.202	0.202
	T = 1	174.0	177.0	2.881	2.920		

5.2 Example 1B - laminated tube

In this example we consider a laminated tube. The lay-up is denoted by $[0/(20^*)_2/0]_T$. Explicitly stated, the top half of the tube has a lay-up given by $[0/(20)_2/0]_T$ and the bottom half $[0/(-20)_2/0]_T$. The elastic constants of the ply material were same as in Example 1A. The forces applied are similar to the previous example. The results are presented in Table 2. Again one notices that the agreement between the analytical results and FEA results is excellent. The shear center distance specified by e_y/L is smaller, *i.e.*, the shear center is closer to the tube center, for the laminated tube compared to the 20-degree lamina in Example 1A, because the laminate includes some 0-degree plies. The reduction in the effective coefficient of mutual influence due to the presence of 0-degree plies reduces the shear center distance also.

Table 2: results for tubes made of two different composite laminates. The lay-up for the top half of the tube is $[0/20_2/0]_S$; for the bottom half $[0/-20_2/0]_S$

Length L (mm)	Load F_z (N) T (N-mm)	Tip deflection $w_0(L)$ $\left(10^{-6}\text{ mm}\right)$		Tip rotation $\psi_x(L)$ (10^{-6} Radians)		Shear Center e_y/L	
		FEA	Analytical	FEA	Analytical	FEA	Analytical
200	F_z = 1	4,462	4,254	25.23	25.49	0.0820	0.0820
	T = 1	25.23	25.49	1.539	1.555		
300	F_z = 1	14,610	14,350	56.83	57.36	0.0820	0.0820
	T = 1	56.8	57.36	2.31	2.332		

5.4 Experimental validation

An experimental method for quantifying e_y/L was developed. A special apparatus was constructed to load the tip with an adjustable torque. The experimental set-up is shown in Figures 7 and 8. Digital image correlation (DIC) was used to measure tip rotation and deflection. From these measurements shear center values were determined as the length of moment arm that results in bending absent twisting. Repeating this process for different shaft lengths and orientations allowed for a final e_y/L measurement for the given design. Steps of the experiment were repeated to reduce the various uncertainties in these measurements. The experiment utilized three dimensional DIC, a vice to simulate the rigid boundary of a cantilever, an adjustable moment arm on which to load the specimen, and the means to manufacture composite shaft specimens. The results were compared against finite element and analytical predictions. The final average experimental e_y/L for all four shafts was 8% higher than what the analytical method and FEA predicted, Table 3.

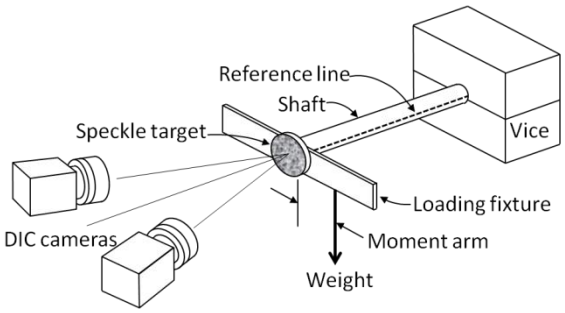

Fig. 7 Schematic of the experimental set-up

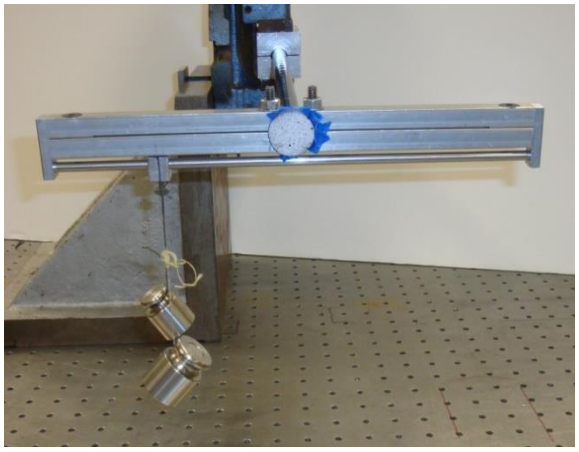

Fig. 8 Experimental set-up

Table 3: Comparison of shear-center distances using various methods

Method	Experimental	Analytical	FEA
e_y/L (mm/mm)	0.099	0.092	0.092

6 SUMMARY

An analytical model is presented for thin walled composite tubes subjected to a combination of bending and torsion. The methods are applied to a novel design of composite tubes with lay-ups in the top and bottom halves of the cross section. Due to the difference in lay-ups, the tube exhibits strong bend-twist coupling and the shear center is at a distance from the geometric center of the tube. The shear center distance is independent of the tube radius but proportional to the length of the tube and the effective coefficient of mutual influence of the laminates. The results are verified using finite element analysis and experimental testing. The excellent agreement in results suggests that the assumptions made in the analytical model are reasonable and correct.

REFERENCES

[1] S.E. Rohde, P.G. Ifju, B.V. Sankar, and D.A. Jenkins, Experimental investigation of bend-twist coupled cylindrical shafts, *Composite, Hybrid, and Multifunctional Materials*, **4**, 2015, pp. 117-124

[2] S.E. Rohde, P.G. Ifju, B.V. Sankar, and D.A. Jenkins, Experimental testing of bend-twist coupled composite shafts, *Experimental Mechanics*, under review

[3] C. Rao, and W.S. Chan, Analysis of laminated composite tapered tubes, *Proceedings of the American Society for Composites (ASC)23rd Technical Conference, Memphis, TN, September 9-11, 2008*, Paper 154.

[4] R. F. Gibson, Principles of Composite Material Mechanics, Ed. 3, CRC Press, Boca Raton, FL, 2012.